

## Report

# Optogenetic and Electrical Microstimulation Systematically Bias Visuospatial Choice in Primates

Ji Dai,<sup>1</sup> Daniel I. Brooks,<sup>1</sup> and David L. Sheinberg<sup>1,\*</sup>

<sup>1</sup>Department of Neuroscience, Brown University, Providence, RI 02912, USA

## Summary

Optogenetics is a recently developed method in which neurons are genetically modified to express membrane proteins sensitive to light, enabling precisely targeted control of neural activity [1–3]. The temporal and spatial precision afforded by neural stimulation by light holds promise as a powerful alternative to current methods of neural control, which rely predominantly on electrical and pharmacological methods, in both research and clinical settings [4, 5]. Although the optogenetic approach has been widely used in rodent and other small animal models to study neural circuitry [6–8], its functional application in primate models has proven more difficult. In contrast to the relatively large literature on the effects of cortical electrical microstimulation in perceptual and decision-making tasks [9–13], previous studies of optogenetic stimulation in primates have not demonstrated its utility in similar paradigms [14–18]. In this study, we directly compare the effects of optogenetic activation and electrical microstimulation in the lateral intraparietal area during a visuospatial discrimination task. We observed significant and predictable biases in visual attention in response to both forms of stimulation that are consistent with the experimental modulation of a visual salience map. Our results demonstrate the power of optogenetics as a viable alternative to electrical microstimulation for the precise dissection of the cortical pathways of high-level processes in the primate brain.

## Results

Our experiments focused on the role that the lateral intraparietal area (LIP) plays in the selection of salient targets for saccadic eye movements. Previous studies indicate that neurons in this cortical area respond to both the presentation of visual stimuli in localized regions of space [19, 20] and saccade planning [21–23], a combination that has been characterized as forming a “salience map” of visual space [24, 25]. In the current study, we hypothesized that the artificial activation of a local population of LIP cells could systematically perturb this salience map, biasing choices under conditions that require the animal to make a decision about where to look. We therefore trained two monkeys to perform a saccade task in which they learned to look toward a target stimulus (see Figure 1). In “single” trials (one-third of the trials), the target (T) appeared alone, in one of six locations equally spaced around the center of the screen, at an eccentricity of 7° visual angle. In the remaining “paired” trials, the target was shown with a distractor (+) presented 180° away (see Figure 1A). In both trial types, monkeys were rewarded

for making a saccade to the target after fixating a central spot (Figure 1A).

To modulate activity in LIP, we used either optical or electrical microstimulation. To obtain optogenetic control, we physiologically identified visual regions of LIP (Figure S1 available online) and then transfected cells in this area with AAV5-CaMKIIa-C1V1 (E122T/E162T)-TS-EYFP, a viral construct that expresses the red-shifted excitatory opsin C1V1 and mainly targets excitatory cells [26, 27]. After transfection, single- and multiunit activity in this area was reliably modulated via the delivery of green light across a wide range of frequencies and optical powers (Figures 1D and S2).

To test whether electrical stimulation or C1V1-mediated optogenetic activation of LIP neurons could affect decision making, we picked sites of strong spatial selectivity (SSI > 0.33; see Supplemental Experimental Procedures) after identifying the most effective receptive field location based on visual responses. For optogenetic experiments, we also sought regions with clear optical modulation (OMI > 0.2; see Supplemental Experimental Procedures). For a single run of the target selection task (576 trials), half of the trials were pseudorandomly selected to be stimulated with a continuous 200 ms light pulse (optogenetic experiments) or a train of biphasic electrical pulses lasting up to 200 ms (electrical experiments) (Figure 2).

For optogenetic experiments, we first mapped the preferred receptive field (RF) of an LIP neuron (Figure 2A) and then recorded both the neural response (Figure 2B) and behavior (Figure 2C) in both the unstimulated and stimulated conditions for all target locations. By convention, our analyses use the angle relative to the RF location to represent each possible target location. The strong neural modulation in stimulated trials was accompanied by a systematic bias in the monkey’s choices. Data from a single experiment of Monkey J (Figure 2C) demonstrates both increased accuracy at the RF and decreased accuracy at the anti-RF location in paired trials. For electrical microstimulation experiments, the procedure was almost identical, with the light stimulation being replaced by current delivery, as illustrated in Figure 2E. For this example experiment (from Monkey I), the RF was mapped as shown Figure 2D, and the effect on accuracy is shown in Figure 2F. Here again, the artificial modulation in activity shifted the monkey’s performance in favor of the targets appearing in the RF, at the expense of those located in the anti-RF location.

To assess the effects of the two forms of stimulation, we performed 40 experiments with optogenetic modulation (21 from Monkey J and 19 from Monkey I) and 45 experiments with electrical microstimulation (24 from Monkey J and 21 from Monkey I). The effects on task accuracy for every experiment are plotted in Figure 3 (only paired trials are shown because accuracy for both conditions was at the ceiling for single trials). In the center of each plot we show the spatial tuning curves determined prior to running the spatial choice discrimination task. For visualization purposes, these curves have been rotated to align each experiment’s RF location to the most common RF location for each animal (i.e., bottom right for Monkey I and upper left for Monkey J). The six

\*Correspondence: [david\\_sheinberg@brown.edu](mailto:david_sheinberg@brown.edu)

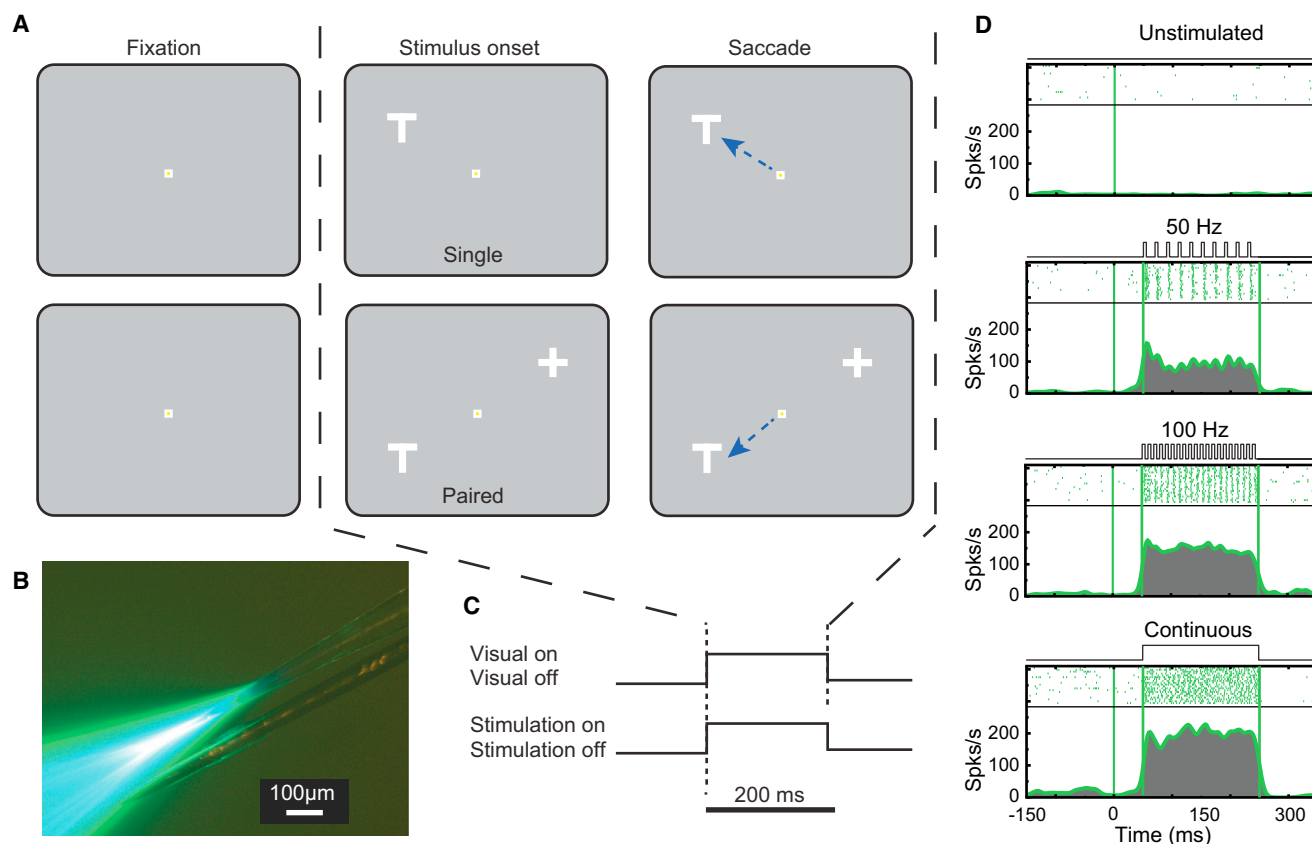


**Figure 1. Experimental Design**

(A) Behavioral task: at one of six locations (at 7° visual eccentricity), a target “T” appeared alone (top, single trials) or with a distractor “+” that appeared at 180° away (bottom, paired trials). In both conditions, monkeys were rewarded for making a saccade to the T after briefly fixating a central spot. (B) Recording optrode: a tapered fiber was glued to a standard tungsten electrode. An image taken in photoluminescent dye demonstrates that, via a staggered construction, the light from this fiber illuminated the tip of the electrode. (C) Stimulation protocol during the optical stimulation trials: a 200 ms light pulse was delivered simultaneously with the visual stimulus onset. (D) A comparison of the optogenetic modulation by different frequencies of light stimulation of a single LIP neuron (see also [Figure S2](#)).

surrounding subplots (also RF rotated) show results for each paired target configuration, as denoted by the insets above. Performance is depicted in the scatterplots, which show performance in the stimulated condition (x value) plotted against performance in the unstimulated condition (y value). The average performance across sessions for stimulated (green) and unstimulated (red) trials is indicated on the right of each plot. Below are the p values of two-tailed paired t tests (complete repeated-measures model described below). [Figures 3A](#) and [3B](#) show effects caused by optogenetic stimulation for Monkey I and Monkey J, respectively. When the target was presented at the RF, activity modulation by light significantly increased accuracy by 10% in Monkey I ( $p = 0.002$ ) and 8% in Monkey J ( $p = 0.028$ ). When the target was presented at the anti-RF location, optical stimulation decreased Monkey I's accuracy by approximately 5% ( $p = 0.05$ ). For Monkey J, the decrement at the anti-RF location was more variable but was highly robust at a location 60° away (15%,  $p < 0.001$ ). We note that, corresponding to the large negative effect at this location, there was strong positive effect (8%,  $p = 0.008$ ) in the opposite direction (60° clockwise from RF location). These “off-RF” effects could be a result of the relatively broader spatial tuning for cells recorded in Monkey J's recording experiments compared to those from Monkey I,

which made a precise definition of a single RF location more difficult.

The corresponding effects caused by electrical microstimulation for the two animals are shown in [Figures 3C](#) and [3D](#). For Monkey I, microstimulation caused an increment in performance of about 8% ( $p = 0.03$ ) for targets at the RF location and about 6% decrement ( $p = 0.06$ ) for the anti-RF location. For Monkey J, electrical microstimulation effects were clear at both the RF (14% increment,  $p = 0.001$ ) and anti-RF (11% decrement,  $p = 0.001$ ) locations.

To directly compare the two types of stimulation, we conducted a repeated-measure ANOVA on the accuracy shifts observed due to stimulation at the RF (between-session factor) and anti-RF (within-session factor). This analysis indicated no significant difference between optical and electrical stimulation (in Monkey I,  $F(1,38) = 0.022$ ,  $p = 0.88$ ; in Monkey J,  $F(1,43) = 2.70$ ,  $p = 0.11$ ; and in a data set pooled across animals to address possible power issues,  $F(1,83) = 1.59$ ,  $p = 0.21$ ).

We also measured the effect of stimulation on the monkey's saccadic reaction times (RTs) by subtracting RTs for unstimulated trials from RTs for stimulated trials. These are plotted in the center of each panel in [Figure 4](#) (also RF, rotated as in [Figure 3](#)). Session-by-session data of the RT effects are shown in

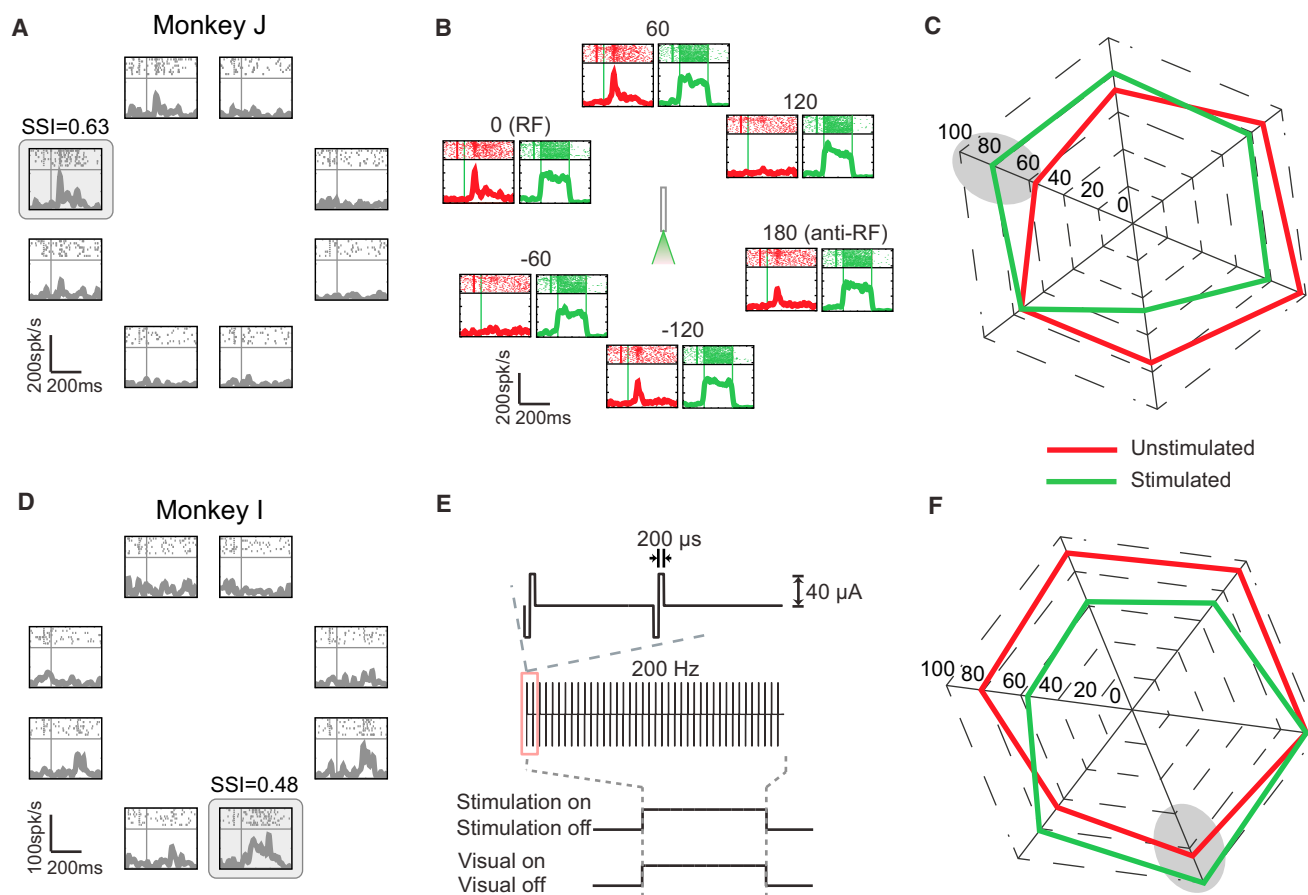


Figure 2. Example Optogenetic and Electrical Microstimulation Experiments

(A)–(C) refer to data from a single optogenetic experiment in Monkey J. (D)–(F) refer to data from a single electrical microstimulation experiment in Monkey I. (A) Each neuron's receptive field was mapped by measuring neural activity to a single spot flashed peripherally in one of eight directions; the RF (highlighted by a gray square) was identified as the location that elicited the maximal response (see [Supplemental Experimental Procedures](#)). RF specificity was measured by calculating a spatial selectivity index (SSI = 0.63 for this neuron). (B) Neural responses from the same cell in (A) during unstimulated (red) and stimulated (green) paired trials with targets presented at the six possible locations. The target location that matches the RF is labeled as 0°; other locations are spaced by 60° increments and labeled with their angular distance from the RF. Because these data come from paired trials, visual responses at anti-RF locations were evoked by the presence of the distractor appearing at the RF. (C) Accuracy in performing the visuospatial discrimination task plotted in polar coordinates corresponding to each target location for unstimulated (red) and stimulated (green) conditions, with the RF indicated by a gray region. (D) RF mapping for this experiment's neuron, as in (A), with SSI = 0.48. (E) Schematic of the electrical microstimulation protocol, which consisted of 200  $\mu$ s, 40  $\mu$ A biphasic current presented at 200 Hz gated by the visual stimulus. (F) Accuracy on trials with or without electrical microstimulation, using the same conventions as in (C).

**Figure S3.** For these data, we analyzed correct responses for both the single and paired trials. For the single-target condition with optogenetic stimulation, we found no significant effect on RT for either monkey (blue data in [Figures 4A](#) and [4B](#)). For the paired condition, optogenetic stimulation sped both monkeys' choices when the target was presented at the RF (purple in [Figures 4A](#) and [4B](#); 5.92 ms for Monkey I,  $p = 0.01$ ; 4.39 ms for Monkey J,  $p = 0.033$ ) but did not significantly affect RTs for targets at any other location.

Electrical microstimulation revealed a somewhat different picture; whereas a similar effect of speeding responses was observed at the RF location, an even larger slowing of saccades was observed in the anti-RF ([Figures 4C](#) and [4D](#)). This anti-RF interference was true for both single trials (blue in [Figures 4C](#) and [4D](#)), in which responses to targets located in the anti-RF were slowed by 8.04 ms ( $p = 0.007$ ) in Monkey I and 8.25 ms ( $p < 0.001$ ) in Monkey J, and paired trials (purple in [Figures 4C](#) and [4D](#)), in which anti-RF responses were slowed by

8.31 ms ( $p = 0.005$ ) for Monkey I and 8.81 ms ( $p = 0.003$ ) for Monkey J. Thus, in contrast to optical stimulation, electrical stimulation exerted its strongest influence by significantly slowing reaction times on trials in which the target appeared away from the RF.

Because computational models of the visual salience map have been described as a winner-take-all process, highly sensitive to the insertion of extra stimulation [28], we looked for any evidence of a speed-accuracy tradeoff that might occur if the computational process was delayed. However, there was no evidence in either type of stimulation that increased accuracy was associated with RT slowing; in fact, both monkeys showed strong negative correlations between accuracy and reaction time across sessions at both the RF (Monkey I:  $r = -0.43$ ,  $p = 0.051$ ,  $n = 21$  sessions; Monkey J:  $r = -0.75$ ,  $p < 0.001$ ,  $n = 24$  sessions) and the anti-RF (Monkey I:  $r = -0.67$ ,  $p < 0.001$ ; Monkey J:  $r = -0.81$ ,  $p < 0.001$ ) for electrical stimulation sessions.

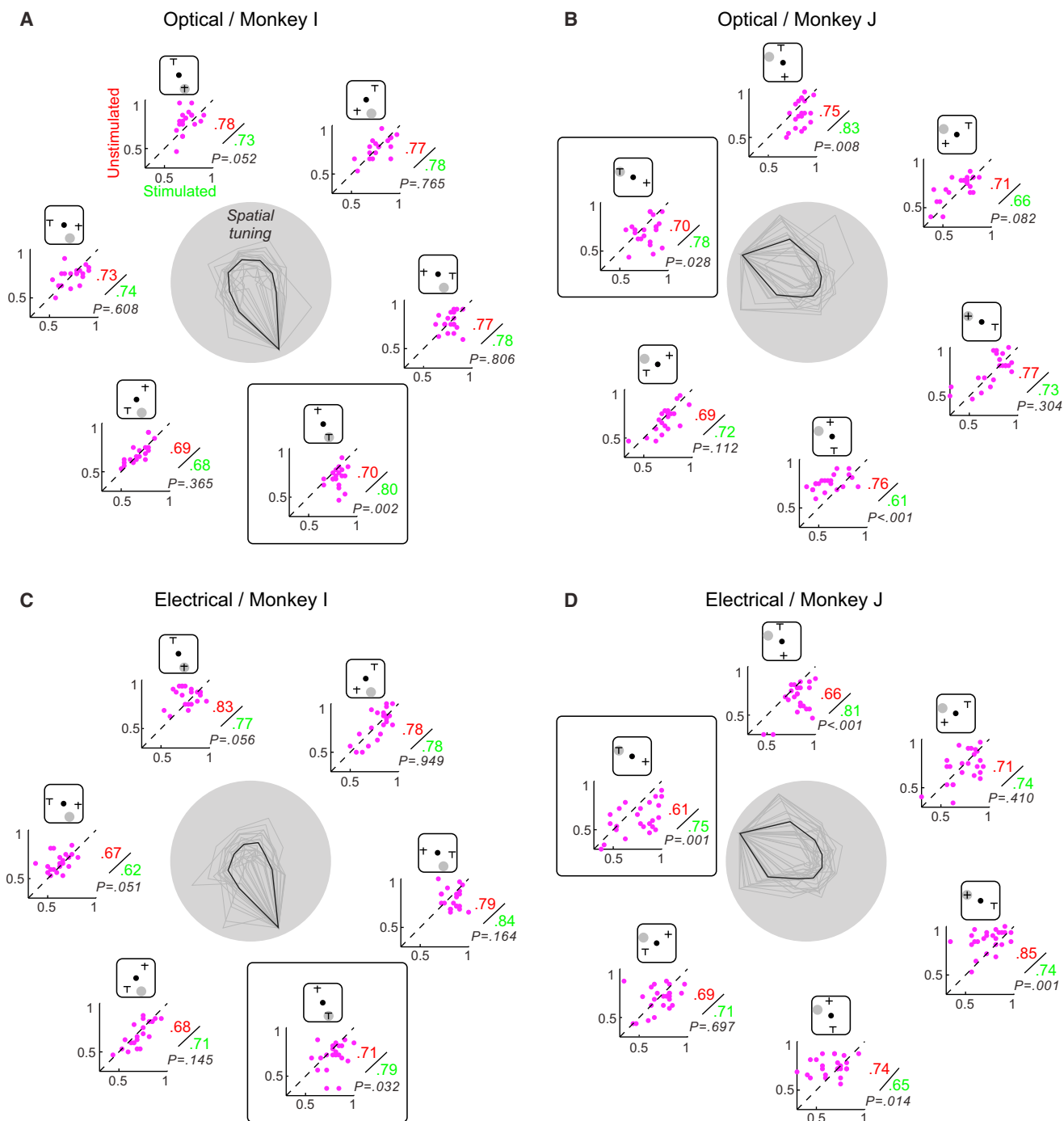


**Figure 3. Optogenetic and Electrical Microstimulation Affects Behavioral Choice**

(A) Accuracy during each optogenetic experiment for Monkey I. In the center we show spatial tuning curves that have been rotated to align each experiment's RF to the most frequently observed RF (bottom right, as highlighted by the square), with a bold curve representing mean spatial tuning. Discrimination performance at each possible target location (also RF rotated, as denoted by the inset) during each experiment is shown by scatterplot, with the x and y axes representing proportion of correct performance for the stimulated and unstimulated conditions, respectively. The average performance across sessions for unstimulated (red) and stimulated (green) trials are indicated adjacent to the plot, and the p values below are the results of two-tailed paired t tests. The same conventions are used for (B)–(D).

(B) Accuracy during each optogenetic experiment for Monkey J.

(C) Accuracy during each electrical microstimulation experiment for Monkey I.

(D) Accuracy during each electrical microstimulation experiment for Monkey J. (Note that, for visualization purposes, the few performance values falling below 0.3 are clipped on the corresponding axes.)

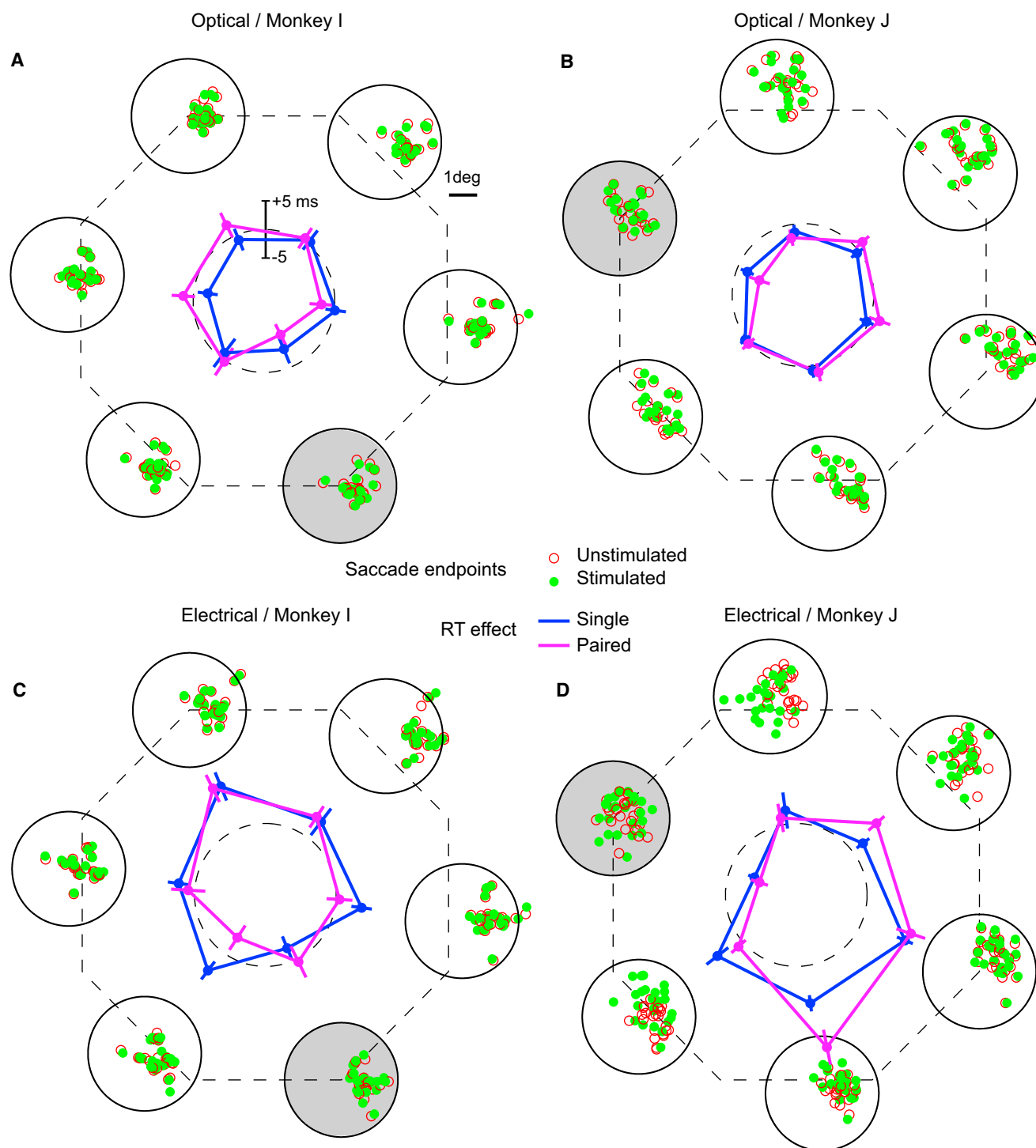


Figure 4. The Effect of Optogenetic and Electrical Microstimulation on Reaction Time and Saccade Endpoints

Each panel shows the average difference in reaction time between the stimulated and unstimulated trials (center) and physical locations of saccade endpoints made to each target (periphery). Each panel has been rotated to align each experiment's RF to the most frequently observed RF (highlighted in gray). (A) RT differences and saccade endpoints during optogenetic experiments in Monkey I. Negative RT differences indicate a faster response during stimulated trials. The dashed reference circle represents no effect. Blue and purple lines represent data from single and paired trials, respectively. Error bars show SEM across experimental sessions. For saccade endpoints, unstimulated and stimulated conditions are shown by open red and filled green circles, respectively, and each circle represents the average position from one session. The dashed octagon indicates the original eight locations used for RF mapping. The same conventions are used for (B)–(D).

(B) RT differences and saccade endpoints during optogenetic experiments in Monkey J.

(C) RT differences and saccade endpoints during electrical microstimulation experiments in Monkey I.

(D) RT differences and saccade endpoints during electrical microstimulation experiments in Monkey J (see also Figure S3).



Because the monkeys' tasks explicitly required responding by making a saccade, we also looked for any specific effects of either form of stimulation on eye movements. Despite previous reports that indicate that electrical microstimulation in LIP can evoke saccades [29], even for sites showing clear evidence of optical modulation (as in Figures 1D and 2B), we never observed an evoked saccade via either optical stimulation or electrical microstimulation (at the light levels or currents we used). To further investigate any effects of stimulation on saccade execution, we looked closely at saccade trajectories and endpoints (outer plots of each panel in Figure 4; these endpoints were extracted from correct single and paired trials, and each point denotes the mean landing position of one experimental session). Upon initial inspection, it was clear that electrical microstimulation appeared to pull Monkey J's saccade landing point toward the RF for trials in which the target appeared in either of the two adjacent locations (Figure 4D, red versus green circles). By calculating the distance of the endpoint to the RF, we found that the endpoints targeting these two locations were significantly closer to the RF when stimulated ( $0.63^\circ \pm 0.10^\circ$  and  $0.68^\circ \pm 0.10^\circ$  [mean  $\pm$  SEM, henceforth] for single trials,  $0.52^\circ \pm 0.07^\circ$  and  $0.60^\circ \pm 0.10^\circ$  for paired trials,  $p < 0.001$ ,  $n = 24$ ). For the optogenetic experiments, no obvious effect was observed. However, in Monkey J and in only one location ( $-60^\circ$  from RF), we found evidence for an extremely small, but significant, effect for both the single and paired conditions in which the endpoints under stimulation were  $0.11^\circ \pm 0.03^\circ$  (single) and  $0.06^\circ \pm 0.02^\circ$  (paired) closer to the RF ( $p < 0.005$ ,  $n = 21$ ). These average endpoint differences were much smaller than the corresponding effect of electrical microstimulation. We characterized the effect size by computing Cohen's  $d$  and found that the effect sizes by optical stimulation for that particular location were only 0.16 (single) and 0.28 (paired), neither exceeding the generally accepted minimum significant effect size (0.41) [30]; the effects of electrical microstimulation on landing position were 0.90 (single) and 1.58 (paired). In no condition did we see any effects on Monkey I's eye movements. From these analyses, we then conclude that direct effects of optical stimulation on saccade programming in our paradigm seem minimal compared to the effect on choice behavior.

Finally, to demonstrate that the effects of optical stimulation were due to evoked neural modulation and not merely the presentation of light, we conducted 22 further control experiments in Monkey I in which we recorded from sites surrounding the C1V1 injection sites ( $>3$  mm away), for which we saw no physiological effect of neural modulation via light stimulation. During these experiments, we ran the same optogenetic protocol but found no significant effect of stimulation at the RF location on either accuracy or RTs. Direct comparison of the accuracy effects for the real optical stimulation trials (Figure 3A) and the control experiment effects were significant ( $p = 0.04$ ), confirming that the neural modulation of spatially characterized cell populations is essential for affecting behavior in our experiments.

## Discussion

While previous studies have demonstrated clear optogenetic modulation of neural activity in the nonhuman primate, associated effects on behavior have been more difficult to demonstrate [5, 14]. Here, we have shown that optogenetic stimulation in LIP can reliably bias choice in a visuospatial discrimination task. As reviewed by Gerits and Vanduffel [31],

of three previous optogenetic studies in nonhuman primates that have reported behavioral effects of stimulation, two of them have performed this stimulation close to the targeted neural pathway's input (primary visual cortex) [16] or output (the superior colliculus) [17] regions and have assessed behavioral effects using relatively simple behavioral measures, such as either fixation patterns or saccades to single targets. Another recent study in the arcuate sulcus using a visually guided saccade task reported effects on saccade latency [15]. Here, we asked whether the optogenetic approach could be employed in another higher cortical area (LIP) during a more complex decision task involving visual target discrimination and spatial choice. Whereas previous behavioral assays in V1 and SC indicated a direct impact on the oculomotor response [16, 17], we observed no elicited saccades or significant effects on eye movement trajectories by optogenetic stimulation, consistent with previous studies [15]. Instead, we found effects consistent with a bias revealed via choice accuracy between two simultaneously presented targets in addition to a small, but reliable, effect on choice reaction time. These results suggest that optogenetic modulation can reliably bias signals in higher-order structures such as LIP. Given that LIP may act as a "salience map" [24, 25] in selecting spatial locations, our findings are consistent with the idea that optogenetic (and electrical) perturbation of activity in such a visual salience map can alter decisions about where to look next.

To bridge the existing literature on electrical microstimulation and optogenetic modulation, we compared the two approaches directly, using the same task in the same animals (in different sessions). A recent study compared the effects of optogenetic stimulation and electrical microstimulation delivered to the frontal eye fields on evoked eye movements during fixation [18]. These authors found that effects of optogenetic stimulation were generally only observable when accompanying electrical stimulation. In our task, in area LIP, we found that the effect of optical stimulation on choice discrimination performance was quite comparable to that caused by electrical microstimulation, consistent with results from a previous study in LIP using electrical microstimulation [12]. However, optogenetic stimulation does seem to have more specific effects on saccadic reaction times (more localized to the RF location) while having very little effect on eye movement trajectories (Figure 4). This suggests that the optical modulation may have led to more localized perturbation in cortical activity than electrical microstimulation, therefore having a less direct influence on oculomotor behavior, which is consistent with the findings of Ohayon et al. [18]. Furthermore, the ability to directly record the effects of optogenetic activation during stimulation (as seen, e.g., in Figures 1 and 2) provides feedback regarding the causal effect of that stimulation that is extremely difficult to obtain with electrical microstimulation.

In conclusion, our results clearly demonstrate that even in an associative cortical area such as LIP, optogenetics in nonhuman primates can be a powerful tool for controlling behavior. Future refinements of this approach, especially with respect to cell-specific targeting, will likely make it the primary tool of choice in the causal examination of complex neural networks.

## Experimental Procedures

Detailed experimental procedures can be found in [Supplemental Experimental Procedures](#) available online.

## Supplemental Information

Supplemental Information includes Supplemental Experimental Procedures and three figures and can be found with this article online at <http://dx.doi.org/10.1016/j.cub.2013.11.011>.

## Author Contributions

J.D., D.I.B., and D.L.S. designed the experiment; J.D. and D.I.B. performed the injections; J.D. collected the data; J.D. and D.L.S. analyzed the data; J.D., D.I.B., and D.L.S. wrote the manuscript.

## Acknowledgments

We thank John Ghenne for his expert assistance with the animal care and training, the Deisseroth laboratory for graciously providing the viral constructs used in the experiments, and the Nurmikko laboratory for assistance constructing optical devices. We are also grateful to Ilker Ozden for his help with characterizing the power distribution of the light fiber. This work was supported by DARPA REPAIR (N66001-10-C-2010).

Received: September 11, 2013

Revised: October 19, 2013

Accepted: November 2, 2013

Published: December 12, 2013

## References

- Boyden, E.S., Zhang, F., Bamberg, E., Nagel, G., and Deisseroth, K. (2005). Millisecond-timescale, genetically targeted optical control of neural activity. *Nat. Neurosci.* 8, 1263–1268.
- Deisseroth, K. (2011). Optogenetics. *Nat. Methods* 8, 26–29.
- Zhang, F., Wang, L.P., Boyden, E.S., and Deisseroth, K. (2006). Channelrhodopsin-2 and optical control of excitable cells. *Nat. Methods* 3, 785–792.
- Fenno, L., Yizhar, O., and Deisseroth, K. (2011). The development and application of optogenetics. *Annu. Rev. Neurosci.* 34, 389–412.
- Han, X., Qian, X., Bernstein, J.G., Zhou, H.H., Franzesi, G.T., Stern, P., Bronson, R.T., Graybiel, A.M., Desimone, R., and Boyden, E.S. (2009). Millisecond-timescale optical control of neural dynamics in the nonhuman primate brain. *Neuron* 62, 191–198.
- Aravanis, A.M., Wang, L.P., Zhang, F., Meltzer, L.A., Mogri, M.Z., Schneider, M.B., and Deisseroth, K. (2007). An optical neural interface: in vivo control of rodent motor cortex with integrated fiberoptic and optogenetic technology. *J. Neural Eng.* 4, S143–S156.
- Adamantidis, A.R., Zhang, F., Aravanis, A.M., Deisseroth, K., and de Lecea, L. (2007). Neural substrates of awakening probed with optogenetic control of hypocretin neurons. *Nature* 450, 420–424.
- Carter, M.E., Yizhar, O., Chikahisa, S., Nguyen, H., Adamantidis, A., Nishino, S., Deisseroth, K., and de Lecea, L. (2010). Tuning arousal with optogenetic modulation of locus coeruleus neurons. *Nat. Neurosci.* 13, 1526–1533.
- Salzman, C.D., Murasugi, C.M., Britten, K.H., and Newsome, W.T. (1992). Microstimulation in visual area MT: effects on direction discrimination performance. *J. Neurosci.* 12, 2331–2355.
- Schiller, P.H., and Tehovnik, E.J. (2005). Neural mechanisms underlying target selection with saccadic eye movements. *Prog. Brain Res.* 149, 157–171.
- Clark, K.L., Armstrong, K.M., and Moore, T. (2011). Probing neural circuitry and function with electrical microstimulation. *Proc. Biol. Sci.* 278, 1121–1130.
- Hanks, T.D., Ditterich, J., and Shadlen, M.N. (2006). Microstimulation of macaque area LIP affects decision-making in a motion discrimination task. *Nat. Neurosci.* 9, 682–689.
- Opris, I., Barborica, A., and Ferrera, V.P. (2005). Microstimulation of the dorsolateral prefrontal cortex biases saccade target selection. *J. Cogn. Neurosci.* 17, 893–904.
- Diester, I., Kaufman, M.T., Mogri, M., Pashae, R., Goo, W., Yizhar, O., Ramakrishnan, C., Deisseroth, K., and Shenoy, K.V. (2011). An optogenetic toolbox designed for primates. *Nat. Neurosci.* 14, 387–397.
- Gerits, A., Farivar, R., Rosen, B.R., Wald, L.L., Boyden, E.S., and Vanduffel, W. (2012). Optogenetically induced behavioral and functional network changes in primates. *Curr. Biol.* 22, 1722–1726.
- Jazayeri, M., Lindbloom-Brown, Z., and Horwitz, G.D. (2012). Saccadic eye movements evoked by optogenetic activation of primate V1. *Nat. Neurosci.* 15, 1368–1370.
- Cavanaugh, J., Monosov, I.E., McAlonan, K., Berman, R., Smith, M.K., Cao, V., Wang, K.H., Boyden, E.S., and Wurtz, R.H. (2012). Optogenetic inactivation modifies monkey visuomotor behavior. *Neuron* 76, 901–907.
- Ohayon, S., Grimaldi, P., Schweers, N., and Tsao, D.Y. (2013). Saccade modulation by optical and electrical stimulation in the macaque frontal eye field. *J. Neurosci.* 33, 16684–16697.
- Gottlieb, J.P., Kusunoki, M., and Goldberg, M.E. (1998). The representation of visual salience in monkey parietal cortex. *Nature* 391, 481–484.
- Kusunoki, M., Gottlieb, J., and Goldberg, M.E. (2000). The lateral intraparietal area as a salience map: the representation of abrupt onset, stimulus motion, and task relevance. *Vision Res.* 40, 1459–1468.
- Mazzoni, P., Bracewell, R.M., Barash, S., and Andersen, R.A. (1996). Motor intention activity in the macaque's lateral intraparietal area. I. Dissociation of motor plan from sensory memory. *J. Neurophysiol.* 76, 1439–1456.
- Grunewald, A., Linden, J.F., and Andersen, R.A. (1999). Responses to auditory stimuli in macaque lateral intraparietal area. I. Effects of training. *J. Neurophysiol.* 82, 330–342.
- Linden, J.F., Grunewald, A., and Andersen, R.A. (1999). Responses to auditory stimuli in macaque lateral intraparietal area. II. Behavioral modulation. *J. Neurophysiol.* 82, 343–358.
- Bisley, J.W., and Goldberg, M.E. (2003). Neuronal activity in the lateral intraparietal area and spatial attention. *Science* 299, 81–86.
- Goldberg, M.E., Bisley, J.W., Powell, K.D., and Gottlieb, J. (2006). Saccades, salience and attention: the role of the lateral intraparietal area in visual behavior. *Prog. Brain Res.* 155, 157–175.
- Yizhar, O., Fenno, L.E., Davidson, T.J., Mogri, M., and Deisseroth, K. (2011). Optogenetics in neural systems. *Neuron* 71, 9–34.
- Ozden, I., Wang, J., Lu, Y., May, T., Lee, J., Goo, W., O'Shea, D.J., Kalanithi, P., Diester, I., Diagne, M., et al. (2013). A coaxial optrode as multifunction write-read probe for optogenetic studies in non-human primates. *J. Neurosci. Methods* 219, 142–154.
- Itti, L., and Koch, C. (2001). Computational modelling of visual attention. *Nat. Rev. Neurosci.* 2, 194–203.
- Thier, P., and Andersen, R.A. (1998). Electrical microstimulation distinguishes distinct saccade-related areas in the posterior parietal cortex. *J. Neurophysiol.* 80, 1713–1735.
- Ferguson, C.J. (2009). An Effect Size Primer: A Guide for Clinicians and Researchers. *Prof. Psychol. Res. Pr.* 40, 532–538.
- Gerits, A., and Vanduffel, W. (2013). Optogenetics in primates: a shining future? *Trends Genet.* 29, 403–411.